Far-Infrared Properties of Lattice Resonant Modes. II. Stress Effects*

I. G. NOLT† AND A. J. SIEVERS
Laboratory of Atomic and Solid State Physics, Cornell University, Ithaca, New York 14850
(Received 14 June 1968)

The resonant-mode frequency shifts produced by uniaxial stress have been measured for KBr:Li^+ and KI:Ag^+. Relative frequency shifts of up to 15% are observed for stresses of 3 kg/mm^2. For both defect systems, the observed splitting pattern is consistent with a defect center of cubic symmetry; moreover, the absence of low-lying tunneling states implies that the equilibrium position of the respective impurity ion is at the normal K^+ lattice site. The considerable difference between the measured stress coupling coefficients for the defects is taken as evidence that stress shifts of resonant modes reflect the bonding of the particular impurity ion with its neighbors.

I. INTRODUCTION

BECAUSE small impurity ions influence the low-temperature thermal properties of alkali-halide crystals, such defect systems have been actively studied in recent years. One of the current theoretical problems is to find a consistent explanation of the defect-induced energy states of lithium impurity ions substituted into KCl and KBr.

For KCl:Li^+, the experimental situation is fairly clear. Low-temperature measurements of the dielectric constant,[1,2] electrocaloric effect,[3] thermal conductivity,[4] specific heat,[5,6] ultrasonic attenuation,[7] and, more recently, paraelectric resonance[8] all show evidence for a number of defect-induced energy states at about 1°K. Far-infrared absorption measurements[9] show an additional absorption band at 40 cm^{-1} (58°K). The low-lying states have been described by a model in which the lithium ion is displaced from the normal lattice site and tunnels between a number of pocket states located around the normal lattice site.[3,10] The 40-cm^{-1} absorption band is identified with transitions to higher tunneling states.

For KBr:Li^+, on the other hand, measurements of the low-temperature dielectric constant,[11] electrocaloric effect,[12] specific heat,[13] and thermal conductivity[14] show that no low-lying states occur between 0.01 and 10°K. Far-infrared absorption measurements have identified a sharp absorption line which occurs at 16.07 cm^{-1} for $^7Li^+$ and at 17.71 cm^{-1} for $^6Li^+$. These measurements have been described by Kirby *et al.*,[15] hereafter referred to as I. Previously, this absorption line has been cited as evidence of a defect-induced lattice resonant mode with the equilibrium position of the impurity placed at the normal lattice site. Presently, this picture is not in agreement with theoretical minimum-energy-configuration calculations for Li^+ impurities.[16,17]

Matthew was the first to recognize the mechanism whereby an impurity could be in an off-center equilibrium position.[16] With a simple one-dimensional model he demonstrated that the electronic dipoles induced in the lattice by the ionic dipole of the impurity tend to destabilize the impurity ion. Because the polarization interaction and the nearest-neighbor repulsive interaction act in opposite directions, the effective coupling constant of the impurity at the normal lattice site can be either positive or negative. A small positive coupling constant would indicate that the impurity is stable at the normal lattice site but is weakly coupled to the lattice, while a negative coupling constant would indicate that the impurity ion is unstable at the normal lattice site. Matthew's calculations showed that Li^+ in KCl could be unstable at the normal lattice site. Because of the larger electronic polarizability of the

* This work was supported primarily by the U. S. Atomic Energy Commission under Contract No. AT(30-1)-2391; Technical Report No. NYO-2391-77. Additional support was received from the Advanced Research Projects Agency through the Materials Science Center at Cornell University, Report No. 961.
† Present address: Institute for Astronomy, University of Hawaii, Honolulu, Hawaii 96822.
[1] H. S. Sack and M. C. Moriarty, Solid State Commun. **3**, 93 (1965).
[2] A. Lakatos and H. S. Sack, Solid State Commun. **4**, 315 (1966).
[3] G. Lombardo and R. O. Pohl, Phys. Rev. Letters **15**, 291 (1965).
[4] F. C. Baumann, J. P. Harrison, R. O. Pohl, and W. D. Seward, Phys. Rev. **159**, 691 (1967).
[5] R. F. Wielinga, A. R. Miedema, and W. T. Huiskamp, Physica **32**, 1568 (1966).
[6] J. P. Harrison, P. P. Peressini, and R. O. Pohl, *Localized Excitations in Solids*, edited by R. F. Wallis (Plenum Press, Inc., New York, 1968), p. 474.
[7] N. Byer and H. S. Sack, Phys. Rev. Letters **17**, 72 (1966).
[8] R. A. Herendeen, Bull. Am. Phys. Soc. **13**, 660 (1968).
[9] A. J. Sievers, *Elementary Excitations and Their Interactions in Solids* (NATO Advanced Study Institute, Cortina, Italy, 1966), Vol. IV, p. 47.
[10] S. P. Bowen, M. Gomez, J. A. Krumhansl, and J. A. D. Matthew, Phys. Rev. Letters **16**, 1105 (1966); M. Gomez, S. P. Bowen, and J. A. Krumhansl, Phys. Rev. **153**, 1009 (1967).
[11] H. Bogardus and H. S. Sack, Bull. Am. Phys. Soc. **11**, 229 (1966).
[12] G. Lombardo and R. O. Pohl, Bull. Am. Phys. Soc. **11**, 212 (1966).
[13] J. P. Harrison, P. P. Peressini, and R. O. Pohl, Phys. Rev. **171** (1968).
[14] The experiment is described in Ref. 4. The recent specific-heat measurements described in Ref. 13 indicate that the lowest-frequency thermal-conductivity resonance in KBr:Li^+ is not caused by lithium ions.
[15] R. D. Kirby, I. G. Nolt, R. W. Alexander, Jr., and A. J. Sievers, Phys. Rev. **168**, 1057 (1968).
[16] J. A. D. Matthew, Solid State Commun. **3**, 363 (1965); Cornell University Materials Science Center Report No. 373, 1965 (unpublished).
[17] W. D. Wilson, R. D. Hatcher, G. I. Dienes, and R. Smoluchowski, Phys. Rev. **161**, 888 (1967).

KBr lattice an impurity which was unstable in KCl would be more unstable in KBr.

This idea was confirmed by W. D. Wilson *et al.* from computer calculations with a more general three-dimensional model.[17] Using classical crystal forces with a point-ion model, they conclude that in both KCl and KBr the lithium ion should not occupy the normal lattice site.

To understand the absence of low-lying states in KBr:Li^+ and yet be consistent with these lattice theories, it has been proposed that the lithium ion is frozen off-center in KBr.[3,17] Because an infrared-active mode is accessible to optical studies at ~ 17 cm^{-1}, spectroscopic stress-shift measurements can provide definitive data on the defect symmetry. With the Li^+ frozen off center in KBr, the defect would have C_{2v}, C_{3v}, or C_{4v} symmetry, whereas if the defect occupied a normal lattice site, O_h symmetry would occur.

Such stress-shift experiments have become feasible with the development of an interferometric spectrometer in conjunction with a helium-cooled bolometer detector. The first measurements of the KBr:Li^+ resonance revealed easily measurable stress shifts, and showed that the lithium defect had O_h symmetry.[18] As Benedek and Nardelli[19] had predicted large stress shifts for all low-lying modes, stress measurements were then made with KI:Ag^+.

In this paper, we present the results of our completed stress-shift measurements on these two systems. In Sec. II, both the far-infrared interferometer and the stress cryostat are described. In Sec. III, the far-infrared results are presented and compared with the predictions expected for different defect symmetries. The coupling constants of the resonant mode to the other lattice modes consistent with O_h symmetry are then deduced. Section IV first considers the recent off-center model of KBr:Li^+ proposed by Quigley and Das.[20] Next, Matthew's simple lattice model is used to demonstrate how large stress shifts can occur for lattice resonant modes and, finally, the difference between the stress results for KBr:Li^+ and KI:Ag^+ are resolved by some preliminary measurements on NaCl:Cu^+, another resonant-mode system. Our conclusions are then summarized in Sec. V.

II. EXPERIMENT

In these studies of lattice-resonant modes, measurements of the transmission spectrum were required in the frequency range below 30 cm^{-1} of an alkali-halide sample at cryogenic temperatures subjected to a known uniaxial stress. The necessity of making these measurements with a fixed polarization of the radiation increased the usual difficulties associated with signal limitations in this spectral range; nonetheless, fairly accurate stress shifts were obtained by the use of a sensitive Ge detector[21] and an interferometric spectrometer.[22]

The optical arrangement of the interferometric spectrometer is shown in Fig. 1. Basically, it is an $f/1.5$ Ebert-Fastie instrument operated as an aperiodically scanned Lamellar-grating interferometer. The source S is a Hg-arc lamp which has an effective blackbody temperature in the far-infrared of 3000°K.[23] For transmission measurements in the 10–30 cm^{-1} range, the higher-frequency components are filtered from the source output by two 180-μ zero-order gratings, F_1 and F_2, and a 0.8-cm-thick filter of fused quartz F_3. The Lamellar grating G divides the incident collimated beam into two interfering components with an optical path difference Δ equal to twice the groove depth. The resultant zero-order energy focused in the exit slit is channeled to the sample and detector cryostat by a 1.25-cm-diam brass light pipe. The bolometer output, which is measured at optical-path-difference increments of 50 μ, is automatically recorded on punched cards. The measured interferogram is then subsequently processed by a numerical Fourier-transform calculation to yield the transmission spectrum. The full details of this calculation have been given elsewhere.[22]

Figure 2 shows the liquid-helium cryostat containing the crystal-loading platens, polarizer,[24] and Ge bolometer detector. This cryostat was immersed in a pumped He bath at approximately 1.5°K. Helium exchange gas was used to stabilize the crystal at the bath temperature. Sample dimensions were typically 1.5 by 1.5 cm, with a thickness in the propagation direction of the

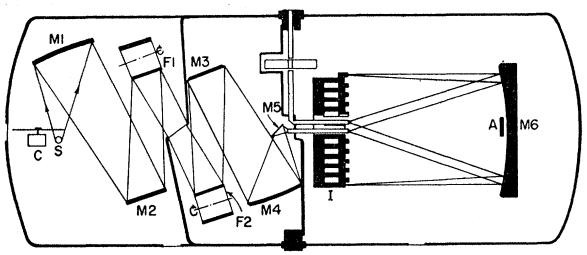

FIG. 1. Optical system of the far-infrared Lamellar-grating interferometer. The optical path is indicated by the arrows. S is the Hg-arc source chopped by a slotted disk C. M designations refer to mirror components. $F1$ and $F2$ are zero-order reflection gratings for filtering purposes, supplemented at $F3$ by transmission filters. The Strong-type Lamellar grating I provides the optical-path difference between the interfering beams. A is a rubber absorbing disk for preventing direct reflection to the exit slit.

[18] I. G. Nolt and A. J. Sievers, Phys. Rev. Letters **16**, 1103 (1966).
[19] G. Benedek and G. F. Nardelli, Phys. Rev. Letters **16**, 517 (1966).
[20] R. J. Quigley and T. P. Das, Phys. Rev. **164**, 1185 (1967).
[21] R. A. Westwig, M. S. thesis, Department of Physics, Cornell University, Materials Science Center Report No. 629, 1967 (unpublished).
[22] I. G. Nolt, Ph.D. thesis, Department of Physics, Cornell University, Materials Science Center Report No. 765, 1967 (unpublished).
[23] R. Papoular, Infrared Phys. 4, 137 (1964).
[24] The polarizing element consisted of a 500-line/cm etched Ni linear grid deposited on a Mylar film obtained from Buckbee-Mears, Inc., Minneapolis, Minn.

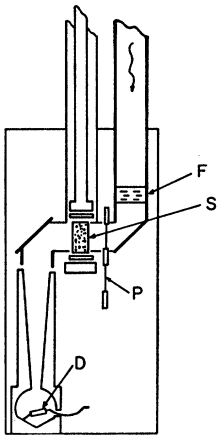

FIG. 2. Schematic sectional view of the stress cryostat. The far-infrared radiation from the spectrometer is conducted to the cryostat down the 1.25-cm-diam brass light pipe, passing in succession through a crystal-quartz filter F (for absorbing the room-temperature radiation), a 500 line/cm polarization screen P, the sample S, to the germanium detector D. The polarizers are attached to a sliding rod extending through the cryostat head, so that either one of two polarization directions could be selected for a given run.

radiation of 0.2–0.4 cm, depending upon the desired absorption strength and ultimate stress. Two different methods were used to apply the compressional force to the crystal sample. A lever and weight arrangement with a mechanical advantage of 4 was used to impose crystal loads of up to 100 kg. A hand hydraulic pump and piston was used to apply higher loads up to the cryostat design limit of 200 kg determined by the strength of the concentric thin-wall stainless-steel pressure rod and sample support tube shown in Fig. 2. The cryostat limit provided maximum sample stresses of 3–5 kg/mm^2, depending upon the crystal cross section.

The usual procedure was to measure the transmission spectrum for a range of low stress values using the lever and weight system and then switch to the hydraulic system for measurements at higher stresses until the cryostat limit was reached or, as sometimes happened, the crystal shattered. At each stress value two polarizations, usually parallel and perpendicular to the stress, could be obtained by the two-position polarizer described in Fig. 2. Each stress-polarization combination required ~45 min to record for an instrumental apodized resolution of ~0.3 cm^{-1} and a signal-to-noise ratio of ~50 in the final computed transmission spectrum.

With this stress cryostat it is not possible to substitute a pure sample in the same run to obtain a normalizing background spectrum in a direct fashion. Instead, the background intensity was either synthesized by comparing the shifted and unshifted transmission profiles or by measuring the transmission of a crystal quartz "sample" in a separate experiment.

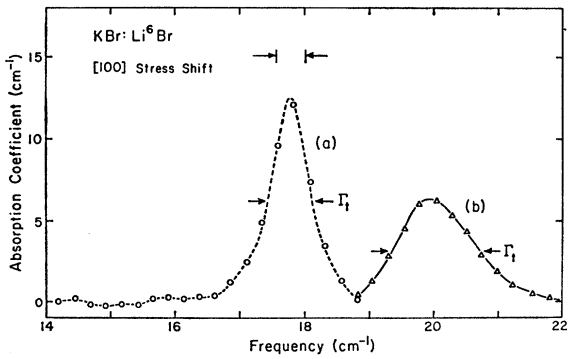

FIG. 3. KBr:Li^6 Br absorption coefficient for E||P[100]. Because of the large frequency shift, each curve can be used to define the background intensity level for the other one. The instrumental resolution bandwidth of 0.43 cm^{-1} is shown by the arrows. For the zero-stress results [curve (a)] the half-width is measured to be 0.7 cm^{-1} and the integrated line strength 10.4±1 cm^{-2}. Subjected to a [100] stress of 3.7 kg/mm^2 [curve (b)], these same two parameters are 1.4 cm^{-1} and 9.6±1 cm^{-2}, respectively.

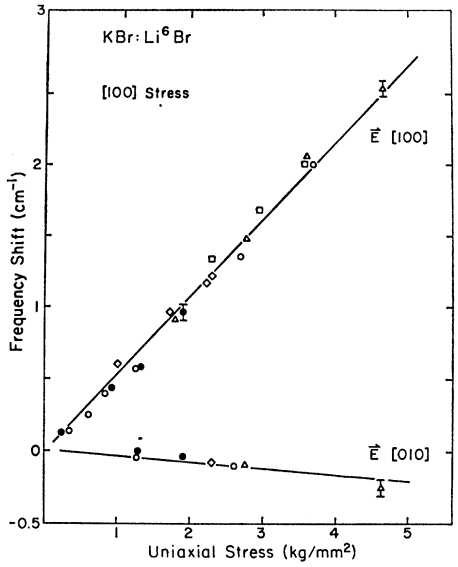

FIG. 4. KBr:Li$^+$ frequency shift induced by [100] stress. The results of three different KBr:Li^6 Br and one KBr:Li^7 Br sample (indicated by ◇) are shown here. The zero-stress frequencies are 17.71 and 16.07 cm^{-1}, with the lower frequency for the heavier isotope. No significant difference between the two isotopes Li^6 and Li^7 can be detected. The solid circles show results for the static-weight system of loading. The higher-stress determinations were obtained with the hydraulic method as discussed in the text. The reproducibility appears consistent with the estimated precision for the frequency determinations of ±0.05 cm^{-1}. The slope values for the two polarizations are tabulated in Table I.

The stress samples, in all cases, were obtained from single-crystal boules grown by the Kyropoulos procedure with 0.05 mole% LiBr added to the melt for the KBr:Li$^+$ specimens and 0.5% AgI for the KI:Ag$^+$ samples. The impurity content was somewhat critical, since the sample-thickness range was restricted by stress-loading considerations. For applying a [100] stress, the samples were simply cleaved to the proper size. For [110] samples, the end faces were hand-sanded at the proper orientation relative to the {100} cleaved surfaces. The [111] stress samples were roughly cut to size using a string saw from a {100} cube so as to yield a finished surface, after some hand polishing, having (111), (1$\bar{1}$0), and (1$\bar{2}$1) faces.

III. EXPERIMENTAL RESULTS

A. Stress-Induced Effects

In spectroscopic stress experiments, the three major quantities of interest are the number of components of the band for different stress and polarization directions, the magnitude of each shift, and the changes, if any, in the absorption strength of the shifted line. The usual procedure is to measure the stress splittings by observing the absorption bands for a symmetry-limited number of different crystallographic stress and polarization combinations.

1. KBr:Li⁺

Measurements on KBr:Li⁺ were made with the uniaxial stress **P** in one of three crystallographic directions, [110], [100], or [111]. The largest frequency shift in all cases was observed for a [100] stress and a parallel polarization of **E**, where **E** denotes the electric field vector of the radiation. The absorption line invariably broadened upon shifting to higher frequencies, with the amount of broadening varying as much as 25% between runs with different samples. At least part of the broadening results from a nonuniform compressional stress, and this experimental problem has prevented any meaningful linewidth-dependence measurements.

To measure changes in the integrated absorption strength, the absorption coefficient was computed and the area under the absorption line was compared at various stress levels. The result for a stress of 3.7 kg/mm² is shown in Fig. 3. The change in the integrated absorption coefficient or dichroism appears to be less than the experimental error of about 5% at 1.5°K. No measurable change in the absorption strength has been obtained. This conclusion is consistent with no detection of dichroism (<5%) for the other $\mathbf{E}\perp\mathbf{P}$ [100] polarization, not shown, where the frequency shift is small enough to allow a direct comparison of the stressed and unstressed transmission profiles. In addition, the other stress-polarization combinations revealed no stress-induced changes in the integrated absorption strength.

In Fig. 4, the center frequency data are plotted as a function of the uniaxial stress in the [100] direction for KBr: $^6Li^+$ and, also, for one run with KBr: $^7Li^+$. The polarization directions are indicated with their respective results. No significant difference in shift was resolved between the two lithium isotopes, but with the limited data on the heavier isotope, a difference in slope as large as 10% could have escaped detection. Figure 5 shows the frequency-shift results for [110] and [111] stress on KBr: $^6Li^+$. For later analysis, the important parameters are the slopes $\Delta\omega/\Delta P$, and these quantities are tabulated in Table I for $^6Li^+$.

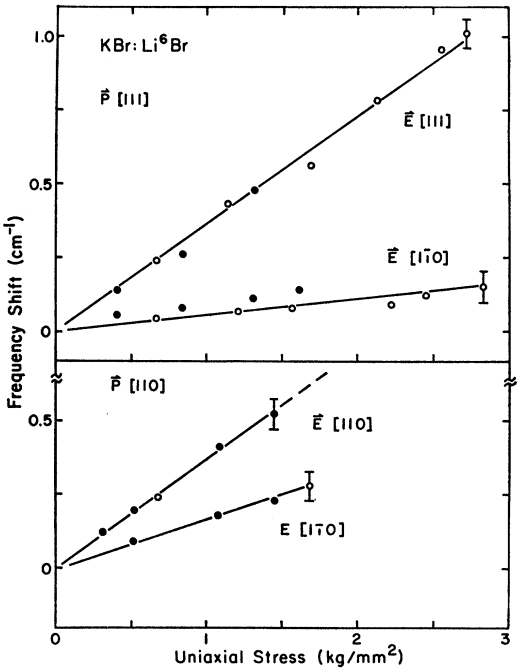

FIG. 5. KBr:Li⁺ frequency shift induced by [110] and [111] stress. The upper figure pertains to two polarizations relative to a [111] stress and the lower to similar results for a [110] stress. Note the change in scales relative to the previous figure. The [111] experiment was an exceptionally low-noise run. As before, the solid circles denote the use of the static-weight method for stressing the crystal. The four experimental slope values are shown in Table I.

TABLE I. Tabulation of experimental stress-shift results. The values shown in parentheses are those predicted on the basis of the italicized results, and they provide a check on the internal consistency of the measurements.

Stress **P**	Polarization **E**	$-\Delta\omega/\Delta P$	Experimental $-(\Delta\omega/\Delta P)$ (cm^{-1} mm^2/kg) KBr:Li⁺	KI:Ag⁺
[100]	[100]	$A(S_{11}+2S_{12})+4B(S_{11}-S_{12})$	*0.54 ±0.04*	*0.74±0.05*
[100]	[010]	$A(S_{11}+2S_{12})-2B(S_{11}-S_{12})$	*−0.04 ±0.02*	*−0.22±0.03*
[110]	[110]	$A(S_{11}+2S_{12})+B(S_{11}-S_{12})+\frac{1}{2}CS_{44}$	0.37 ±0.04 (0.4)	0.24±0.04 (0.22)
[110]	[1$\bar{1}$0]	$A(S_{11}+2S_{12})+B(S_{11}-S_{12})-\frac{1}{2}CS_{44}$	0.17 ±0.02 (0.11)	0.30±0.02 (0.30)
[111]	[111]	$A(S_{11}+2S_{12})+\frac{2}{3}CS_{44}$	*0.37 ±0.02*	*0.09±0.02*
[111]	[1$\bar{1}$0]	$A(S_{11}+2S_{12})-\frac{2}{3}CS_{44}$	*0.055±0.02*	*0.13±0.02*

2. $KI:Ag^+$

The experiments on KI:Ag^+ paralleled those described previously for KBr:Li^+. Some difficulty was encountered with a depression in the background transmission which coincided closely with the zero-stress KI:Ag^+ absorption at ~ 17.3 cm^{-1}. Consequently, the center frequencies could not be determined directly from the transmission spectrum, but were obtained from the absorption coefficient by referring the KI:Ag^+ transmission to a crystal-quartz transmission spectrum in the same system. The results for a [100] stress of 3.3 kg/mm^2 are shown in Fig. 6. The difference in center frequencies between the $\mathbf{E}\|[100]$ and $\mathbf{E}\perp[100]$ polarizations is 3.75 cm^{-1}, or a frequency shift of 20% relative to the unstressed frequency. The shift in center frequency as a function of uniaxial stress is shown in Fig. 7 for the [100] case and Fig. 8 for the [110] and the [111] applied stress. The six experimental slopes from these data are tabulated in Table I.

Again, for this defect system at a temperature of 1.5°K no stress-induced changes in integrated absorption larger than an estimated experimental error of $\pm 10\%$ were noted.

B. Analysis

Because the KBr:Li^+ and the KI:Ag^+ absorption lines show similar stress effects, both lattice defect systems will be analyzed together. We intend to consider a number of alternative models for the defect-lattice system and to show how the stress results eliminate some of the alternatives.

Suppose the impurity ion is frozen off-center. The defect symmetry then is C_{2v}, C_{3v}, or C_{4v}, depending on whether the impurity is displaced in the [110], [111], or [100] direction of the alkali-halide lattice. For C_{2v} symmetry, the impurity-mode oscillator states would be nondegenerate in the excited state; however, a stress-induced splitting would still occur because of the 12 equivalent [110] directions in the unstressed cubic crystal. For C_{3v} and C_{4v} defect symmetries, the application of stress may lift both the degeneracy in the excited oscillator state as well as the orientational degeneracy just considered for the C_{2v} defect-symmetry case. Kaplianskii has calculated the number and polarization of stress-shifted transitions for anisotropic centers in cubic lattices.[25,26] Inspection of his results shows that the low symmetry centers always give more components than observed in our stress results. From the number of components observed, our results are consistent only with T_d or O_h symmetry for the defect.[27] An electric field measurement is necessary to eliminate the T_d symmetry possibility unambiguously. A defect with T_d symmetry has not appeared in any of the theoretical models, so this possibility is ignored in this paper.

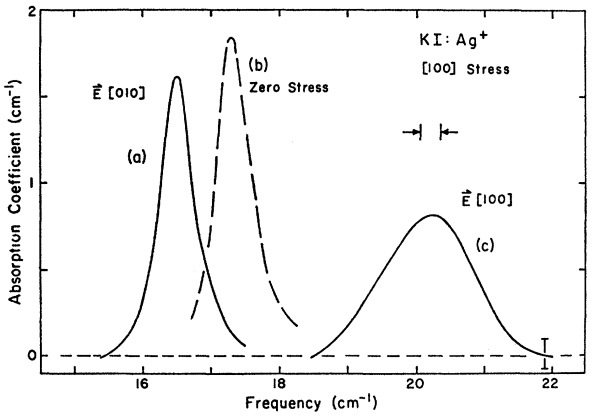

FIG. 6. KI:Ag^+ absorption coefficient for a [100] stress of 3.3 kg/mm^2. This absorption coefficient is calculated relative to a crystal-quartz sample in the same system and shows the largest frequency-splitting observed in these studies. Notice the smaller absorption coefficient values relative to the previous lithium case, and for these results the crystal thickness was 5 mm. The instrumental resolution is 0.3 cm^{-1} and is shown by the arrows above curve (c). The integrated absorption strength was measured to be 1.03, 1.23, and 1.1 ± 0.1 cm^{-2} for curves (a), (b), and (c), respectively.

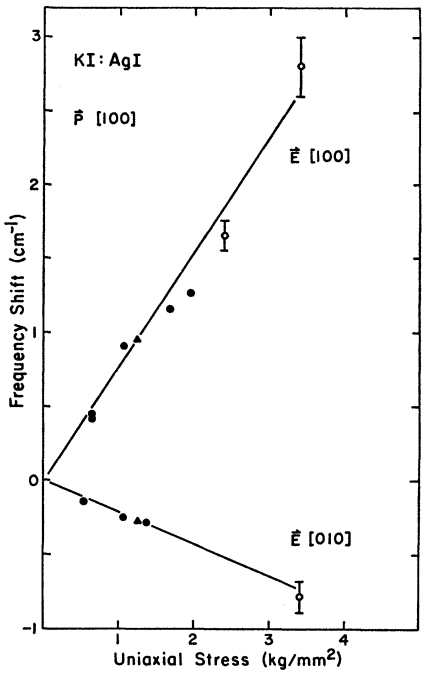

FIG. 7. KI:Ag^+ frequency shift induced by [100] stress. The results for two different samples are shown. Both samples contained Ag ions having the natural isotopic abundance for which the zero-stress frequency is 17.32 cm^{-1} (see Ref. 15). Because of the generally weaker absorption level in the KI:Ag^+ samples, the precision of the frequency determinations is only ± 0.1 cm^{-1}. The two slope values are tabulated in Table I.

[25] A. A. Kaplianskii, Opt. i Spektroskopiya **16**, 1031 (1964) [English transl.: Opt. Spectry. (USSR) **16**, 557 (1964)].
[26] D. B. Fitchen, *Physics of Color Centers*, edited by W. B. Fowler (Academic Press Inc., New York, 1968), Chap. 5.
[27] W. Hayes and H. F. Macdonald, Proc. Roy. Soc. (London) **A297**, 503 (1967).

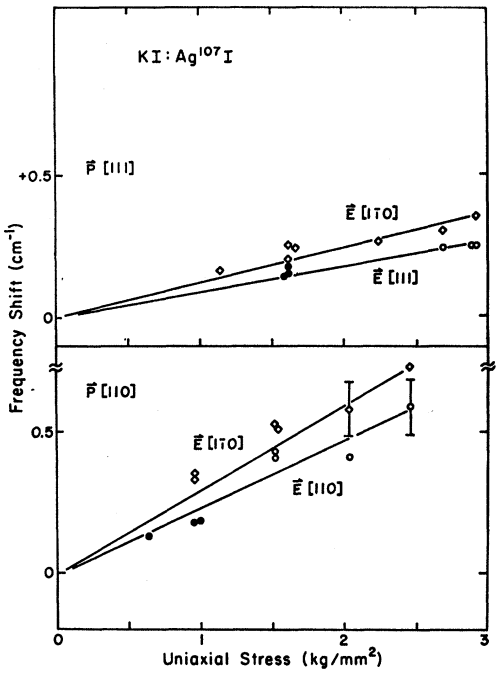

FIG. 8. KI:Ag$^+$ frequency shift induced by [110] and [111] stress. The zero-stress frequency is 17.23 ± 0.02 cm^{-1} for the heavier Ag isotope of mass 109. Note the change in scales relative to the previous figure. The upper figure shows the results for a [111] stress and the lower one is for a [110] case. Both these orientations are consistent in showing a larger frequency shift for the perpendicular-stress-polarization configuration than for the parallel case. Again, the slope values are tabulated in Table I.

The lithium or silver impurity with O_h symmetry is described by two models: the on-center defect or the off-center defect with tunneling between different pocket states. An A_{1g}-to-T_{1u} transition can occur for either model, and so can be consistent with our stress results. Because the stress shifts are on the order of the sample temperature or larger, the absence of dichroism implies that the T_{1u} state must be the excited state in the oscillator transition.

For the off-center impurity model, in addition to the A_{1g} ground state a number of low-lying levels are to be expected, in analogy with the KCl:Li$^+$ system. As applied stress changes the splittings within the ground multiplet, the absorption strengths should change because of population changes in the different tunnel levels. Since no structure in the absorption line or dichroism in the line strength of any component has been found in either KBr:Li$^+$ or KI:Ag$^+$ (see Figs. 3 and 6), our stress results indicate that either the impurity occupies a stable equilibrium position at the normal lattice site or the absorption line which is observed in the far infrared is the transition to the *lowest* optically active tunneling state. For either model, then, the problem is to calculate the influence of uniaxial stress on an s- to p-state transition.

Following previous treatments[10,28,29] of this problem for electronic s- to p-state transitions, the stress perturbation H' is assumed to be a linear function of the local Cartesian strains, i.e.,

$$H'=\sum_{i,j} h_{ij}\epsilon_{ij}. \tag{1}$$

It is more convenient to write the perturbation in terms of the strain coefficients, which transform according to the irreducible representations of the octahedral point group. Equation (1) is rewritten as

$$H'=\sum_{\mu\nu} h_\mu(\Gamma^\nu)\epsilon_\mu(\Gamma^\nu), \tag{2}$$

where

$$\begin{aligned}
\epsilon_1(A_{1g})&=-(S_{11}+2S_{12})P,\\
\epsilon_1(E_g)&=-(2\alpha^2-\beta^2-\gamma^2)(S_{11}-S_{12})P,\\
\epsilon_2(E_g)&=-(\beta^2-\gamma^2)(S_{11}-S_{12})P,\\
\epsilon_1(T_{2g})&=-S_{44}\alpha\beta P,\\
\epsilon_2(T_{2g})&=-S_{44}\beta\gamma P,\\
\epsilon_3(T_{2g})&=-S_{44}\alpha\gamma P,
\end{aligned}$$

and $h_\mu(\Gamma^\nu)$ are constants defining the coupling of the defect to the lattice. P is the uniaxial stress having direction cosines α, β, and γ relative to the [100] crystal axis and the S_{ij} are the stiffness constants. Physically, the only modes which interact with the excited state of the lattice oscillator of T_{1u} symmetry are the long-wavelength distortions of A_{1g} (spherical), E_g (tetragonal and orthorhombic), and T_{2g} (trigonal) symmetry. Three coupling coefficients A, B, and C then determine the dependence of the resonant-mode frequency upon the lattice strains.

The calculation of the coupling coefficients to the different symmetry strain components has been discussed by various authors. Gebhart and Maier[28] evaluate these matrix elements by using symmetry arguments which hold for certain stress-polarization directions. Schnatterly[29] derives equivalent expressions from the method of moments. Perhaps more closely related to our problem is the evaluation of the matrix elements in the tunneling approximation by Gomez *et al.*[10] The resulting relations between the applied stress, frequency shift, and coupling coefficients are reproduced in Table II.

With the experimentally determined slopes italicized in Table I, three quantities are calculated which define the frequency shift in terms of applied stress. These are $A(S_{11}+2S_{12})$, $B(S_{11}-S_{12})$, and $C\,S_{44}$. Our experimental values for these quantities are tabulated in Table II. To calculate the coupling coefficients, the crystal compliances S_{ij} must be evaluated. The compliances are known for the pure crystal but not for the defect crystal.

[28] W. Gebhardt and K. Maier, Phys. Status Solidi **8**, 303 (1965).
[29] S. E. Schnatterly, Phys. Rev. **140**, 1364 (1965).

TABLE II. Stress coupling coefficients for KBr:Li^+ and KI:Ag^+.

	KBr:Li^+	KI:Ag^+
	Experimental results (in cm^{-1} mm^2/kg)	
$A(S_{11}+2S_{12})$	0.16±0.02	0.10±0.03
$B(S_{11}-S_{12})$	0.10±0.01	0.16±0.02
CS_{44}	0.31±0.04	−0.04±0.02
Coefficients calculated using host-crystal compliances [in cm^{-1}/(unit strain)]		
$A(A_{1g})$	830±100	390±90
$B(E_g)$	360± 40	510±70
$C(T_{2g})$	170± 30	− 15±10
Coefficients calculated using local compliances calculated in Ref. 31 [in cm^{-1}/(unit strain)]		
$A(A_{1g})$	480	225
$B(E_g)$	312	246
$C(T_{2g})$	144	266

Recently, Elliott *et al.*[30] have shown in a general way how the strains induced locally around a defect by an applied stress can be related to the elastic strains in the perfect crystal. Using this idea, Benedek and Nardelli[31] have carried through an explicit calculation with a short-range perturbation of a substitutional impurity in an NaCl-type lattice. This specific calculation is probably of limited value because a short-range perturbation is not consistent with the properties of an ionic lattice, where long-range electric forces come into play.[32] Recently, the Lifshitz treatment has been extended by Page and Strauch[33] to include changed long-range Coulomb forces into a tractable solution. In principle, then, the compliances are known but in practice there still remains the unsettled question of how the stiffness constants of the host crystal should be modified to account for a softening of the lattice in the neighborhood of the impurity. In Table II, we show coupling coefficients A, B, and C, which are calculated with the host-crystal compliances[34] and also the calculated results of Benedek and Nardelli.

IV. DISCUSSION

In addition to the stress results, a variety of different experiments have demonstrated that low-lying states do not occur in KBr:Li^+. Probably the most conclusive experimental results are those of Harrison *et al.*,[13] where the low-temperature specific heat was used as a probe. No low-energy states between 0.01 and 10 cm^{-1} were found which depended on lithium concentration. If the lithium ion is assumed to be off-center in KBr as suggested by Quigley and Das,[20] then the lowest tunneling transition must be identified with the absorption line in the far infrared at 16.07 for $^7Li^+$ and 17.71 for $^6Li^+$. This measured isotope shift which was described in I does not satisfactorily fit the tunneling model. For a three-dimensional model, Gomez-Rodriguez[35] found that the isotope shift could be only roughly fit if a barrier of 3.5 cm^{-1} was assumed between pocket states. Because the zero-point energy of the oscillator (~8.5 cm^{-1}) is much larger than the barrier energy, the off-center model merges with the simpler anharmonic-oscillator model in this limit. The description of the absorption line observed in KBr:Li^+ and also in KI:Ag^+ as a lattice resonant-mode transition is a natural extension of his solution.

We now show how a simple lattice resonant-mode model will explain the unusually large stress shifts which have been reported here. For this purpose we use a particularly tractable dynamical model,[36] where the lattice is assumed to consist of point masses coupled harmonically to nearest neighbors. The unperturbed force constant K couples neighboring masses m to each other, and the perturbed force constant K' couples the impurity mass m' to the nearest neighbors. In this model, the noncentral force components are set equal to the central components. In the low-frequency region, where the resonant frequency ω_r of the T_{1u} mode is much less than the Debye frequency ω_D, the perturbed nearest-neighbor force constant is related to ω_r by

$$\mu=\frac{(\omega_D/\omega_r)^2-3\lambda}{\lambda-2-(\omega_D/\omega_r)^2}, \tag{3}$$

where $\mu=K'/K-1$ and $\lambda=m'/m-1$.

Using the observed zero-stress resonant-mode frequencies for Li^+ and Ag^+, Eq. (3) is solved giving $K'/K=0.0063$ for KBr:Li^+ and $K'/K=0.14$ for KI:Ag^+.

The substitution of these values into the appropriately differentiated form of Eq. (3) gives the following simple relation between the frequency shift and the nearest-neighbor force-constant change:

$$d\omega_r/\omega_r=\beta dK'/K', \tag{4}$$

where $\beta=0.53$ for Li^+ and $\beta=0.50$ for Ag^+. The force-constant change can be related to the lattice-constant change by noting that the A_{1g} hydrostatic coupling coefficient gives the resonant-mode frequency shift per unit volume change. The dependence of the frequency upon the lattice constant can be written as

$$\frac{3A}{\omega_r}=-\frac{d\ln\omega_r}{d\ln a}=-\frac{a}{\omega_r}\frac{d\omega_r}{da}, \tag{5}$$

where a is the lattice constant and A is the hydrostatic coupling coefficient as defined earlier.

[30] R. J. Elliott, J. A. Krumhansl, and R. H. Merrett, *Localized Excitations in Solids*, edited by R. F. Wallis (Plenum Press, Inc., New York, 1968), p. 709.
[31] G. Benedek and G. F. Nardelli, Phys. Rev. **167**, 837 (1968).
[32] J. A. Krumhansl, *Localized Excitations in Solids*, edited by R. F. Wallis (Plenum Press, Inc., New York, 1968), p. 17.
[33] J. B. Page and D. Strauch (Ref. 32), p. 559.
[34] J. K. Galt, Phys. Rev. **73**, 1460 (1948); M. H. Norwood and C. V. Briscoe, *ibid.* **112**, 45 (1958).
[35] M. Gomez-Rodriguez, Ph.D. thesis, Physics Department, Cornell University, Materials Science Center Report No. 910, 1968 (unpublished).
[36] A. J. Sievers and S. Takeno, Phys. Rev. **140**, A1030 (1965).

Substituting Eq. (4) into Eq. (5), we find

$$\frac{3A}{\omega_r} = -\beta \frac{dK'}{da} \frac{a}{K'}. \tag{6}$$

To show that this quantity becomes very large for lattice resonant modes, we identify K' with an effective nearest-neighbor force constant as first proposed by Matthew.[16]

As a first approximation of the eigenvector appropriate to the resonant mode, we assume that all ions except the impurity move together as expected for a very-long-wavelength acoustic mode.[37] The impurity ion, on the other hand, is taken to be π out of phase with the rest of the lattice, and to produce an oscillating electric dipole moment in an ionic crystal. In the c.m. frame, the impurity ion position is described by coordinates (x,y,z).

Assume that the impurity ion moves only in the x direction; then the potential energy of the crystal $V(x)$ will change according to the expansion

$$V(x) = V_0 + \tfrac{1}{2}K'x^2. \tag{7}$$

To estimate K', the following interatomic potentials are introduced: the point-ion electrostatic potential, the Born-Mayer potential between nearest neighbors, and the electronic polarization potential from the lattice. An explicit numerical calculation of the resultant potential has been given by Matthew.[16] Our interest is mainly in the functional form of the various contributions. The nearest-neighbor force constant varies with lattice constant in the following manner: For the Born-Mayer term

$$K_1'(a) \propto f[\exp(-a/\rho)], \tag{8}$$

for the nearest-neighbor electronic polarization

$$K_2'(a) \propto -f(1/a^6), \tag{9}$$

and for the electronic polarization from the rest of the lattice

$$K_3'(a) \propto -f(1/a^3). \tag{10}$$

Because the electronic polarization terms, Eqs. (9) and (10), tend to destabilize the impurity, the net force constant

$$K' = K_1' + K_2' + K_3' \tag{11}$$

can be very small for an accidental cancellation. Such a cancellation no doubt occurs for KBr:Li^+ and also KI:Ag^+. Although K' may be small, dK'/da will be dominated by the rapid variation of the Born-Mayer term; in other words, $K' \ll K$, but $dK'/da \approx dK/da$. Returning to Eq. (6), our argument above shows that the numerator will be roughly the same for all impurities, while the denominator goes to zero as the effective-force constant goes to zero. In practical terms, resonant-mode frequency shifts of a wave number or two can be expected in stressed alkali-halide crystals regardless of the resonant-mode frequency itself. This fact was first recognized by Benedek and Nardelli.[19]

So far, we have emphasized the similarity of the experimental results obtained for KBr:Li^+ and KI:Ag^+; there are also some significant differences which we now consider. Unfortunately, because our knowledge of the local elastic constants is still very limited, we can make only qualitative remarks about the coupling coefficients A, B, and C defined earlier.

For an isotropic oscillator model, such as described by Eq. (3), where the dynamics of the impurity can be resolved into independent x, y, and z components, the B coupling coefficient should be one-half of the magnitude of the A coefficient.[22]

This behavior corresponds reasonably well to that observed for KBr:Li^+, where $A \approx 2.4B$. The U-center local-mode transition[38] and also the F-center electronic transition[28] show similar behavior for the stress coefficients. On the other hand, for the resonant mode in KI:Ag^+, A is significantly less than B. We interpret this to mean that noncentral force components are more important for KI:Ag^+ than for any of the above-mentioned cases. Klein[39] has suggested that the noncentral components may be correlated with the tendency of the Ag^+ ion to form covalent bonds. Fortunately, another element from the same column of the periodic table as Ag^+, Cu^+, produces a low-frequency resonant mode in NaCl. Some stress measurements of a more limited nature have been carried out on this defect system.[40] The results are encouraging; the ratio of A to B for NaCl:Cu^+ is very similar to that found for KI:Ag^+. Thus a fairly consistent picture emerges for the coupling coefficient which gives evidence of appreciable noncentral force components for KI:Ag^+ (and NaCl:Cu^+) but not in KBr:Li^+. From a more general view, the stress-coupling coefficients appear to reflect the bonding of a particular impurity ion with its neighbors.

V. SUMMARY

Improvements in far-infrared instrumentation have made possible the investigation of some new properties of defect-induced lattice vibrations with characteristic frequencies which lie within the acoustic continuum of the host crystal. The main effort here was devoted to the measurement of the resonant-mode frequency shifts induced by uniaxial stress in KBr:Li^+ and also KI:Ag^+. The results of our investigation are summarized below.

The symmetry of the defect center is cubic for Li^+ and Ag^+. Since no evidence of low-lying tunneling states has been seen, we conclude that the equilibrium position

[37] A. J. Sievers, *Localized Excitations in Solids*, edited by R. F. Wallis (Plenum Press, Inc., New York, 1968), p. 29.

[38] B. Fritz, J. Gerlach, and U. Gross (Ref. 32), p. 504.

[39] M. Klein, *Physics of Color Centers*, edited by W. B. Fowler (Academic Press Inc., New York, 1968), Chap. 7.

[40] Our preliminary results show that $A \approx 100$, $B \approx 550$, and $C \approx 0$ for NaCl:Cu^+. A complete study of the stress coupling coefficients for NaCl:Cu^+ is being made by G. Busse, Physikalisches Institut der Universität, Freiburg im Breisgau, Germany.

of the impurity ion is at the normal lattice site for both cases. The theoretical models of Wilson *et al.*[17] and of Quigley and Das[20] are not consistent with these results. Because low-frequency lattice resonant modes are particularly sensitive to the details of the interatomic potential, this disagreement between theory and experiment is not too surprising. No doubt the study of resonant modes will lead to better potential models. The investigation of stress-induced frequency shifts surely will continue to be an important probe of the interatomic potential because the frequency shifts are unusually large: Relative shifts between various polarization components are about 20% for stresses of 5 kg/mm^2. The magnitude of the frequency shifts is understandable in terms of the large energy change associated with a small overlap of ions with filled electron shells.

The major difficulty in interpreting stress shifts quantitatively is still the unknown local elastic constants. For KBr:Li^+, the resonant mode appears to be coupled most strongly to spherically symmetric distortions and progressively less to those of tetragonal and trigonal symmetry. On the other hand, the resonant mode in KI:Ag^+ is most strongly coupled to tetragonal distortions of the surrounding lattice and progressively less to those of spherical and trigonal symmetry. Similar results were obtained for the resonant modes in NaCl:Cu^+. Apparently the appreciable noncentral force components in these latter two cases arise from partially covalent Ag^+ or Cu^+ bonds. Because of this difference in the coupling coefficients between Li^+, on the one hand, and Ag^+ or Cu^+ on the other, the stress coupling coefficients must probe mainly the effective potential of the impurity ion itself in the lattice resonant mode.

ACKNOWLEDGMENTS

The authors acknowledge helpful discussions with Dr. J. A. Krumhansl, Dr. R. O. Pohl, Dr. J. B. Page, and Dr. G. Benedek. We also wish to recognize the crystal-growing assistance rendered by D. Bower, R. Gray, and G. Schmidt.

PHYSICAL REVIEW VOLUME 174, NUMBER 3 15 OCTOBER 1968

Photoconductivity in Colored Potassium Chloride*

FRANCES H. CHAPPLE, GERHARD LEHMANN, AND ALLEN B. SCOTT
Department of Chemistry, Oregon State University, Corvallis, Oregon 97331
(Received 1 April 1968)

The photoconductive sensitivity, during the course of bleaching F centers in KCl, was found to vary in much the same way for excitation in the M and N bands as for excitation in the F band, from which it appears that the major effect of bleaching is to decrease the lifetime of photoelectrons. The lifetime of photoelectrons giving rise to the secondary photocurrent was approximately linear with the sensitivity. From the second-order decay of photocurrent, the trapping cross section of α centers at room temperature was found to be about 10^{-13} cm^2. Shallow traps were investigated by means of current glow and isothermal untrapping. Two sets were identified, with depths of about 0.60 and 0.68 eV; the concentration and characteristics vary somewhat between samples.

DURING the bleaching of F centers by means of light which they absorb, in additively colored KCl, some pronounced changes in photoconductive sensitivity have been reported.[1–3] At room temperature, the usual result is a decrease in photoconductive sensitivity which is relatively much greater than is the decrease in F-band height. Markham,[4] and also Hardtke, Scott, and Woodley[2] attributed the reduced sensitivity to the production, during bleaching, of α centers (i.e., negative-ion vacancies) which were assumed to have greater electron-trapping cross section than the traps ultimately filled by the liberated F-center electrons.

Recent work on the photochemical formation of F-center aggregates, and also upon the trapping of electrons by α centers, indicates that the above interpretation is in need of reexamination. It is now clear[5] that the chief products of bleaching at room temperature, the M, R, and N centers, are clusters of two, three, and probably four F centers, respectively; the formation of these products does not result in the production of new α centers. Moreover, during the photochemical process the mobile species appears to be the α center[6] which implies that even those α centers formed may not remain long as isolated traps but rather migrate to join in more complex centers. There is also good

* Supported by the National Science Foundation.
[1] J. J. Oberly, Phys. Rev. 84, 1257 (1951).
[2] F. C. Hardtke, A. B. Scott, and R. E. Woodley, Phys. Rev. 119, 544 (1960).
[3] M. Hirai and A. B. Scott, J. Chem. Phys. 40, 2864 (1964).
[4] J. J. Markham, Phys. Rev. 86, 433 (1952).
[5] See, for example, J. Schulman and W. D. Compton, *Color Centers in Solids* (The Macmillan Co., New York, 1962).
[6] C. Delbecq, Z. Physik 171, 560 (1963).